Basu, Deepankar

Working Paper

A note on the theory and empirics of the Goodwin model

Working Paper, No. 2024-7

Provided in Cooperation with:
Department of Economics, University of Massachusetts

Suggested Citation: Basu, Deepankar (2024) : A note on the theory and empirics of the Goodwin model, Working Paper, No. 2024-7, University of Massachusetts, Department of Economics, Amherst, MA,
https://hdl.handle.net/20.500.14394/54830

This Version is available at:
https://hdl.handle.net/10419/305482

A Note on the Theory and Empirics of the Goodwin Model

A Note on the Theory and Empirics of the Goodwin Model

Deepankar Basu*

September 28, 2024

Abstract

I discuss some theoretical and empirical points about the Goodwin model. First, I offer a simple proof that solution trajectories around the stable critical point in the Goodwin model are closed orbits but not limit cycles. Moreover, in a neighborhood of the stable critical point, the closed orbits are ellipses. Second, I compare the predictions of the Goodwin model with patterns observed in actual annual data for the U.S. economy for the period 1950-2019. I find that the predictions of the model regarding three key aspects of cycles—the amplitude, time period and the direction of motion—are fully or partially at variance with observed data.
JEL Codes: B51.
Key words: Goodwin model; closed orbit.

1 Introduction

The model of cyclical growth proposed by Goodwin (1967) has been seminal in heterodox macroeconomics for the study of cyclical dynamics of capitalist economies (Desai and Ormerod, 1998). It is now part of graduate-level textbook presentations of heterodox macroeconomics.[1]

The Goodwin model consists of a 2-dimensional nonlinear autonomous differential equation system in the employment rate, v, and the wage share, u. Plausible behavioral reasoning can be used to derive the two equations of the Goodwin model, where the growth rate of

*Department of Economics, UMass Amherst. Email: dbasu@umass.edu. I have benefited from comments on an earlier version of this note by Debarshi Das, Thanos Moraitis and Peter Skott.

[1]For instance see Blecker and Setterfield (2019, chapter 2.8) and Skott (2023, chapter 9.4).

the employment rate is impacted negatively by wage share and the growth rate of the wage share is impacted positively by the employment rate. Thus, the structure of the Goodwin model is formally similar to the Lotka-Volterra predator-prey model used in the study of population biology.

The most interesting and important property of the Goodwin model is that its solution trajectories are *closed orbits* in the phase plane (with the wage share, u, measured on the y-axis and the employment rate, v, measured on the x-axis). This implies that the wage share and employment rate will continuously fluctuate around, but never settle down to, the stable equilibrium. Moreover, Goodwin used a classical perspective in which investment is completely determined by savings out of profits. Hence, there are no demand-side problems. The economic significance of Goodwin's model, therefore, is that it generates perpetual undamped cycles even in the absence of demand fluctuations.

To Goodwin, the existence of closed-orbit solutions of his system was obvious; so, he did not provide any proof of this key claim. Commenting on the solutions, he merely noted that it

> ... can be shown, and indeed is quite obvious, that these solution points lie on a closed, positive curve, B, in u, v space. (Goodwin, 1967, page 56).

Proofs offered by later scholars are either incomplete or complicated.[2] For instance, Flaschel (1984) points out that the proof in Velupillai (1979) was incomplete. Instead, Flaschel (1984, page 68) offers a complete proof which is quite intricate and relies on real analysis.

In this paper, I offer a short proof using Liapunov's second method and another simpler but longer one using basic calculus. This establishes the well-known result that all trajectories are closed orbits, and implies that local trajectories, i.e. those starting near the equilibrium points, are closed orbits too. Moreover, the nonlinear system (defining the Goodwin model) is *locally linear* near the stable critical point. Thus, the linearized system

[2]For instance, the textbook treatment in Blecker and Setterfield (2019) does not offer a proof.

gives us a valid approximation of the behavior of the nonlinear system near the stable critical point. Thus, I also study the behavior of the the Goodwin model in a neighborhood of the stable critical point.

We get an interesting result if we restrict ourselves to domains close to the stable critical value: near the stable critical value, the closed orbits are *ellipses* on the plane. Thus, not only do we know that solution trajectories are closed orbits, we even know their exact shapes. Moreover, since every trajectory is a closed orbit, there are no limit cycles.

While the Goodwin model presents an intuitively appealing explanation of some cyclical phenomena in capitalist economies, it is also necessary to investigate whether its predictions matches patterns observed in actual data. To do so, I compare time series plots and connected XY plots of the two variables of the Goodwin model, the employment rate and the wage share, with actual data for the U.S. economy. The patterns in actual data are not matched very well by the predictions of the Goodwin model beyond the fact of cyclical fluctuations. Predictions of the model about three important features of the cycle—time period, the amplitude and direction (clockwise or counter-clockwise)—are not supported very strongly by the data.

The rest of this note is organized as follows: in section 2, I present a short outline of the Goodwin model; in section 3, I study the stability properties of the stable equilibrium and identify its critical value; in section 4, I show that the solution trajectories are closed orbits; in section 5, I carry out a very simple empirical analysis; in section 6, I conclude.

2 The Goodwin Model

For ease of comparison, I will use Goodwin's notation. Readers who are familiar with the model can directly go to equation (6) and (7). For others, I will derive the equations of the model quickly.

Unless otherwise noted, all variables appearing in the model are continuous functions of time. For any variable x, $\widehat{x} = \dot{x}/x$ will denote its growth rate and $\dot{x}$ will denote the derivative of x with respect to time, t.

Let w and a denote the real wage rate and labor productivity, respectively. Hence, $u = w/a$ denotes the wage share. Let l and n denote the level of employment and labor force, respectively, so that $v = l/n$ denotes the employment rate. Goodwin proposed a real wage-Phillips curve linking the real wage rate and the employment rate as follows,

$$\widehat{w} = -\gamma + \rho v, \quad (\gamma > 0, \rho > 0), \tag{1}$$

where γ and ρ are parameters. The real wage-Phillips curve captures the idea that the size of the reserve army of labor has an impact on how much real wage growth workers can enforce. When the reserve army of labor is large (or when v is small), the workers are not able to ensure wage growth; in fact, when $v < v^* = \gamma/\rho$, the real wage starts falling.[3] On the other hand, when the reserve army becomes smaller (with increasing v), i.e. when $v > v^* = \gamma/\rho$, the bargaining power of workers increase and they are able to ask for and get a higher real wage rate growth. For every percentage increase in the employment rate, workers are able to secure $\rho > 0$ percentage growth in the real wage rate.

Goodwin assumed a constant rate of growth of labor productivity, a, given by $\alpha > 0$. Since $\widehat{u} = \widehat{w} - \widehat{a}$, combining the real wage-Phillips curve with constant labor productivity growth, we we get the first equation of the Goodwin system:

$$\widehat{u} = -(\alpha + \gamma) + \rho v.$$

Goodwin assumed a fixed capital-output ratio, $\sigma = k/q$, where k and q denote the capital

[3] In this analysis, $v^* = \gamma/\rho$ can be understood as the threshold employment rate above which the growth rate of real wage becomes positive.

stock and real output, respectively. This implies that the growth rate of output is always equal to the growth rate of the capital stock, i.e. $\widehat{k} = \widehat{q}$. Since labor productivity is given by $a = q/l$, we have

$$\widehat{l} = -\widehat{a} + \widehat{q} = -\alpha + \widehat{q} = -\alpha + \widehat{k}, \tag{2}$$

where I have used the constancy of labor productivity growth and constancy of the level of the capital-output ratio (which implies $\widehat{k} = \widehat{q}$).

Using a classical perspective, Goodwin assumed that all profits are saved and invested, so that (ignoring depreciation),

$$\dot{k} = (1 - u)\, q,$$

which implies that

$$\widehat{k} = \frac{\dot{k}}{k} = \frac{(1-u)\, q}{k} = \frac{(1-u)}{\sigma}.$$

Using this in (2), we get

$$\widehat{l} = -\alpha + \frac{(1-u)}{\sigma}. \tag{3}$$

Since $v = l/n$, is the employment rate, we have

$$\widehat{v} = \widehat{l} - \widehat{n}.$$

Goodwin assumed that the labor force, n, grows at the constant rate $\beta > 0$. Using the expression for $\widehat{l}$ in (3), we get the second equation of the Goodwin system:

$$\widehat{v} = -\alpha + \frac{(1-u)}{\sigma} - \beta.$$

We can now summarize the above discussion by the following 2-dimensional autonomous

nonlinear differential equation system,

$$\dot{v} = \left[\left(\frac{1}{\sigma} - \alpha - \beta\right) - \frac{1}{\sigma}u\right] v, \tag{4}$$

$$\dot{u} = \left[-\left(\alpha + \gamma\right) + \rho v\right] u, \tag{5}$$

to capture the Goodwin model. In this model, v (employment rate) and u (wage share) are the endogenous variables; the other variables are exogenous parameters.

3 Stability Analysis of the Goodwin Model

3.1 Reparametrized version

To analyze the Goodwin model, I will use the following reparametrized version

$$\dot{v} = \left[\eta_1 - \theta_1 u\right] v \tag{6}$$

$$\dot{u} = \left[-\eta_2 + \theta_2 v\right] u \tag{7}$$

where all the parameters appearing in this reparametrized version are assumed to be fixed in value and strictly positive (Goodwin, 1967, page 56):

$$\eta_1 = \left(\frac{1}{\sigma} - \alpha - \beta\right) > 0, \theta_1 = \frac{1}{\sigma} > 0; \eta_2 = \left(\alpha + \gamma\right) > 0, \theta_2 = \rho > 0. \tag{8}$$

3.2 Two critical points

The differential equation system in (6) and (7) has two critical points (i.e. equilibria), which can be found by solving $\dot{v} = \dot{u} = 0$: $(v = 0, u = 0)$ and $(v = \eta_2/\theta_2, u = \eta_1/\theta_1)$. To study the

stability property of these critical points, we need to evaluate the Jacobian matrix

$$J(v,u) = \begin{bmatrix} \eta_1 - \theta_1 u & -\theta_1 v \\ \theta_2 u & -\eta_2 + \theta_2 v \end{bmatrix}, \tag{9}$$

at the critical points.

At the first critical point, $(0,0)$, we have

$$J(0,0) = \begin{bmatrix} \eta_1 & 0 \\ 0 & -\eta_2 \end{bmatrix}$$

Thus, the determinant of $J(0,0)$ is $-\eta_1\eta_2 < 0$. This implies that the two eigenvalue of $J(0,0)$ are real and of opposite signs. Hence, the origin is a *saddle* point (we do not need information about the trace to draw this conclusion). This critical point is not of theoretical interest.

At the second critical point $(\eta_2/\theta_2, \eta_1/\theta_1)$, we have

$$J(\eta_2/\theta_2, \eta_1/\theta_1) = \begin{bmatrix} 0 & -\frac{\eta_2\theta_1}{\theta_2} \\ \frac{\eta_1\theta_2}{\theta_1} & 0 \end{bmatrix}$$

Hence, trace and determinants of $J(\eta_2/\theta_2, \eta_1/\theta_1)$ are 0 and $\eta_1\eta_2 > 0$, respectively. This implies that the two eigenvalue of $J(\eta_2/\theta_2, \eta_1/\theta_1)$ are purely imaginary numbers. Hence, the critical point $(\eta_2/\theta_2, \eta_1/\theta_1)$ is either a center or a spiral point (Boyce and DiPrima, 2009, Table 9.3.1, page 513). If it is the former, then trajectories are closed orbits; if it is the latter, then the trajectories are spirals. In the next section, I will use Liapunov's second method (Boyce and DiPrima, 2009, section 9.6) to show that the critical point $(\eta_2/\theta_2, \eta_1/\theta_1)$ is stable.[4] That will establish that the trajectories are closed orbits.

[4] I offer a longer calculus-based proof in the appendix that does not use Liapunov's second method.

4 Closed-orbit trajectories around the center

4.1 Global behavior

I will use the following reformulated theorem from (Boyce and DiPrima, 2009, page 547).

Theorem 1. *Suppose that the autonomous system in (6) and (7) has an isolated critical point at* $(\eta_2/\theta_2, \eta_1/\theta_1)$*. If there exists a function* V *that is continuous and has continuous first partial derivatives, is positive definite, and for which the function* $\dot{V}$ *(time derivative of* V*) is negative semidefinite on some domain* D *in the* vu*-plane containing* $(\eta_2/\theta_2, \eta_1/\theta_1)$*, then* $(\eta_2/\theta_2, \eta_1/\theta_1)$ *is a stable critical point.*

The differential equation system (6) and (7) has two critical pints, $(0,0)$ and $(\eta_2/\theta_2, \eta_1/\theta_1)$. Since $\eta_2/\theta_2 > 0$ and $\eta_1/\theta_1 > 0$, both are isolated critical points.

Let

$$V(v,u) = \left(\theta_2 v - \eta_2 \ln v - \theta_2 + \eta_2 \ln \frac{\eta_2}{\theta_2}\right) + \left(\theta_1 u - \eta_1 \ln u - \theta_1 + \eta_1 \ln \frac{\eta_1}{\theta_1}\right) \tag{10}$$

denote a Liapunov function. It is easy to see that the Liapunov function is continuous and $V(\eta_2/\theta_2, \eta_1/\theta_1) = 0$. Since $V_v = \theta_2 - \eta_2/v$ and $V_u = \theta_1 - \eta_1/u$, it follows easily that the first partial derivatives, V_v and V_u are continuous and that $V_v(\eta_2/\theta_2, \eta_1/\theta_1) = V_u(\eta_2/\theta_2, \eta_1/\theta_1) = 0$.

Now consider the second derivative of the Liapunov function,

$$V''(v,u) = \begin{bmatrix} V_{vv} & V_{vu} \\ V_{uv} & V_{vv} \end{bmatrix} = \begin{bmatrix} \frac{\eta_2}{v^2} & 0 \\ 0 & \frac{\eta_1}{u^2} \end{bmatrix}. \tag{11}$$

The first and second principal minors of the matrix $V''(v,u)$ are given by $\eta_2/v^2 > 0$ and $\det V''(v,u) = (\eta_1\eta_2)/(v^2u^2) > 0$, respectively. Hence, the matrix $V''(v,u)$ is positive

definite (Binmore, 1991, page 225). By Theorem 19.42 in Binmore (1991, page 227), the Liapunov function (10) has a local minimum at $(\eta_2/\theta_2, \eta_1/\theta_1)$.

Let C denote circle centered at $(\eta_2/\theta_2, \eta_1/\theta_1)$ with radius $\delta > 0$. For a sufficiently small value of δ, $V(v,u) > 0$ on all points of the circle other than the center because $V(\eta_2/\theta_2, \eta_1/\theta_1) = 0$ and it attains a minimum at $(\eta_2/\theta_2, \eta_1/\theta_1)$.[5] Hence, the Liapunov function, V, in (10) is positive definite on C.

Now, let us compute the time derivative of the Liapunov function $V(v,u)$. Using expressions for $\dot{v}$ and $\dot{u}$ from (6) and (7), and the expressions for the first partial derivatives written above, we get

$$\frac{dV(v,u)}{dt} = V_v \frac{dv}{dt} + V_u \frac{du}{dt} = \left(\theta_2 - \frac{\eta_2}{v}\right)[\eta_1 - \theta_1 u]\, v + \left(\theta_1 - \frac{\eta_1}{u}\right)[-\eta_2 + \theta_2 v]\, u = 0.$$

Hence, the time derivative of $V(v,u)$ is negative semi-definite everywhere on the plane, including on the circle, C.

Now, using Theorem 9.61 in Boyce and DiPrima (2009), we can conclude that $(\eta_2/\theta_2, \eta_1/\theta_1)$ is a stable critical point of the differential equation system (6) and (7). This implies that the trajectories are closed orbits in the (v,u) plane.[6]

While the trajectories are closed orbits, they are not limit cycles—because *every* trajectory is a closed orbit and therefore no trajectory converges on to any other trajectory. It is important to recall that not every closed orbit is a limit cycle.[7] "In general, a closed trajectory in the phase plane such that other nonclosed trajectories spiral toward it, either from the inside or the outside, as $t \to \infty$, is called a limit cycle." (Boyce and DiPrima, 2009,

[5] By choosing a small enough value of δ, we can always ensure that $(0,0)$ lies outside the circle, C.

[6] The proofs offered in Simon and Blume (1994, page 706–07) and in Skott (2023, page 254–55) are similar to each other and slightly different from the one presented here. They both show that trajectories are level curves of a convex function of two variables and conclude that the trajectories are closed orbits. To my mind, these proofs remain incomplete unless it is demonstrated that level curves of a convex function are closed curves.

[7] Blecker and Setterfield (2019, page 97) seem to conflate the two.

page 557). Precisely for this reason, the proof in the general case rests partly on showing that there are no limit cycles (Velupillai, 1979; Flaschel, 1984).

4.2 Local behavior

4.2.1 Locally linear system

While the argument in the previous sub-section establishes closed-orbit trajectories of the solution no matter where the system starts (as long as it is in the first quadrant of the plane), it is interesting to also study solution trajectories near the stable critical point. Since all trajectories are closed orbits, so also will be the local ones. But for local trajectories, we can go further and show that they are ellipses. Note that we can legitimately use local trajectories as good approximations of global behavior because the Goodwin model is *locally linear* near the stable critical point (Boyce and DiPrima, 2009, page 509–12).

Definition 1. *A differential equation system*

$$\dot{v} = F(v, u) \tag{12}$$

$$\dot{u} = G(v, u) \tag{13}$$

is locally linear at a critical value (v^*, u^*) if the functions F and G have continuous partial derivatives and the Jacobian matrix evaluated at (v^*, u^*),

$$J(v^*, u^*) = \begin{bmatrix} F_v(v^*, u^*) & F_u(v^*, u^*) \\ G_v(v^*, u^*) & G_u(v^*, u^*) \end{bmatrix}$$

is invertible.

The definition of a locally linear system has two components: continuity of partial derivatives of F and G and invertibility of the Jacobian matrix at the critical point. The first

component ensures that, in a neighborhood of the critical value (u^*, v^*), the nonlinear system (12) and (13) can be well approximated by a linearized version using the Taylor series expansion of functions F and G. The invertibility of the Jacobian matrix at the critical value ensures that the critical value is isolated, i.e. there are no other critical values in a neighborhood of the critical point (just like in a linear system with a nonsingular coefficient matrix).[8]

For the Goodwin model, the first partial derivatives are continuous, as we have seen above. Moreover, the Jacobian matrix (9) of the Goodwin model is invertible at the critical value $(\eta_2/\theta_2, \eta_1/\theta_1)$ because the determinant is $\eta_1\eta_2 > 0$. Hence, the system is locally linear and we will get a good approximation of the system's behavior near this critical value by studying the linearized system. What is additionally interesting is that the local solutions are ellipses, i.e. not only are they closed orbits (which we already know from the global behavior of the system around the center), but their shapes are those of a familiar conic section, the ellipse.

4.2.2 Local trajectories near the stable critical point

In a small neighborhood of the critical point $(\eta_2/\theta_2, \eta_1/\theta_1)$, the 2-dimensional nonlinear differential equation system (6) and (7) can be approximated by the linear system

$$\begin{bmatrix} \frac{d}{dt}\left(v(t) - \frac{\eta_2}{\theta_2}\right) \\ \frac{d}{dt}\left(u(t) - \frac{\eta_1}{\theta_1}\right) \end{bmatrix} = \begin{bmatrix} 0 & -\frac{\eta_2\theta_1}{\theta_2} \\ \frac{\eta_1\theta_2}{\theta_1} & 0 \end{bmatrix} \begin{bmatrix} \left(v(t) - \frac{\eta_2}{\theta_2}\right) \\ \left(u(t) - \frac{\eta_1}{\theta_1}\right) \end{bmatrix}. \tag{14}$$

[8] For a linear n-dimensional system $\dot{x} = Ax$, the only critical value is $x = 0$ if the n-dimensional square matrix A is invertible. For the nonlinear system near the critical point, the invertibility of the Jacobian matrix mimics this condition.

A solution of this linear system is given by

$$v(t) = \frac{\eta_2}{\theta_2} + \frac{\eta_2}{\theta_2} K \cos\left(t\sqrt{\eta_1\eta_2} + \phi\right), \tag{15}$$

$$u(t) = \frac{\eta_1}{\theta_1} + \frac{\eta_1}{\theta_1}\sqrt{\frac{\eta_2}{\eta_1}} K \sin\left(t\sqrt{\eta_1\eta_2} + \phi\right), \tag{16}$$

where K and ϕ are constants that can be determined by initial conditions. That these are valid solutions can be verified by directly differentiating the expressions and plugging them, along with the expression for the solutions themselves, in (14).

Rearranging the solution in (15), we get

$$\cos\left(t\sqrt{\eta_1\eta_2} + \phi\right) = \frac{\theta_2}{\eta_2 K}\left(v(t) - \frac{\eta_2}{\theta_2}\right),$$

and rearranging the solution in (16), we have

$$\sin\left(t\sqrt{\eta_1\eta_2} + \phi\right) = \frac{\theta_1}{\sqrt{\eta_1\eta_2}K}\left(u(t) - \frac{\eta_1}{\theta_1}\right).$$

Since

$$\sin^2\left(\sqrt{\eta_1\eta_2}t + \phi\right) + \cos^2\left(\sqrt{\eta_1\eta_2}t + \phi\right) = 1,$$

on inserting the expression for the sin and cos terms and rearranging terms, we get

$$\frac{\left(v(t) - \frac{\eta_2}{\theta_2}\right)^2}{\left(\frac{\eta_2 K}{\theta_2}\right)^2} + \frac{\left(u(t) - \frac{\eta_1}{\theta_1}\right)^2}{\left(\frac{\sqrt{\eta_1\eta_2}K}{\theta_1}\right)^2} = 1,$$

which is the equation of an ellipse on the (v, u) plane centered at $(\eta_2/\theta_2, \eta_1/\theta_1)$ and parallel to the v and u axes.

Thus, trajectories of the system are traced out by ellipses on the (v, u) plane, which are of course all closed orbits. Different values of K, determined by initial conditions, give

different non-intersecting ellipses. Once K is fixed (by initial conditions), the trajectory is a particular ellipse.

4.3 Direction of motion

As an additional matter, we can determine the direction of the trajectory on the xy plane where employment rate (v) is measured on the x-axis and wage share (u) is measured on the y-axis. To so so, I will consider four special points on any closed orbit around the critical point $(\eta_2/\theta_2, \eta_1/\theta_1)$ and determine the sign of $\dot{v}$ and $\dot{u}$ at those points using (6) and (7).

- For a point that is due East of the critical point $(\eta_2/\theta_2, \eta_1/\theta_1)$, $\dot{v} = 0$ (because $u = \eta_1/\theta_1$) and and $\dot{u} > 0$ (because $v > \eta_2/\theta_2$). Hence, v does not change and u increases. The trajectory points due North.

- For a point that is due North of the critical point $(\eta_2/\theta_2, \eta_1/\theta_1)$, $\dot{v} < 0$ (because $u > \eta_1/\theta_1$) and and $\dot{u} = 0$ (because $v = \eta_2/\theta_2$). Hence, v declines and u does not change. The trajectory points due West.

- For a point that is due West of the critical point $(\eta_2/\theta_2, \eta_1/\theta_1)$, $\dot{v} = 0$ (because $u = \eta_1/\theta_1$) and and $\dot{u} < 0$ (because $v < \eta_2/\theta_2$). Hence, v does not change and u decreases. The trajectory points due South.

- For a point that is due South of the critical point $(\eta_2/\theta_2, \eta_1/\theta_1)$, $\dot{v} > 0$ (because $u < \eta_1/\theta_1$) and and $\dot{u} = 0$ (because $v = \eta_2/\theta_2$). Hence, v increases and u does not change. The trajectory points due East.

Bringing these together, we can conclude that the trajectories move in a counter-clockwise movement on the xy plane where employment rate (v) is measured on the x-axis and wage share (u) is measured on the y-axis. If we instead measure the wage share (u) on the x-axis

and the employment rate (v) on the y-axis, then the trajectories will move in a clockwise direction.

5 Some empirical evidence

In this section, I confront the predictions of the Goodwin model with data for the US economy. To do so, I present two figures, one with actual data and the other with data generated by the Goodwin model.

Figure 1 presents time series and connected XY plots of the employment rate and the wage share, the two variables of the Goodwin model. Employment rate is measured as the ratio of total employment to the total civilian labor force; wage share is measured as the share of labor compensation in GDP at current national prices. Both series are taken from the website of the Federal Reserve Bank of St. Louis.[9]

Figure 2 presents time series plots of the employment rate and the wage share generated by the Goodwin model in (6) and (7) with initial values $v_0 = 0.58$ (employment rate) and $u_0 = 0.66$ (wage share), and the following parameters:

- From 1948 to the current period, the labor force has increased at 0.66 per cent per year in the US; hence, I use $\beta = 0.0066$.

- From 1948 to the current period, output per worker has increased at 0.88 percent per year in the US; hence, I use $\alpha = 0.0088$.[10]

- The average capital-output ratio since the beginning of the 1950s has been 3.71 in the

[9]The employment rate is measured as the ratio of total employment to the total civilian labor force. This is available as the series CIVPART from the website of the Federal Reserve Bank of St. Louis. The wage share is measured as the share of labor compensation in GDP at current national prices. This is available as the series LABSHPUSA156NRUG from the website of the Federal Reserve Bank of St. Louis.

[10]Data for the labor force and the wage share downloaded from the website of the Federal Reserve Bank of St. Louis.

US; hence, I use $\sigma = 3.71$.[11]

- I assume $\rho = 0.25$ and $\gamma = 0.16$; these imply that the threshold employment rate of the real wage Phillips curve is $v^* = 0.64$. This roughly matches the average employment rate in the U.S. economy over the last several decades.

Comparing Figure 1a and 2, we see some similarities and differences. The obvious similarity is the cyclical nature of the time series in both figures, i.e. the time series of the employment rate and the wage share displays cyclical fluctuations in actual data, which is what is predicted by the Goodwin model. Beyond this basic similarity, there are two stark differences.

First, in the actual data (Figure 1a), employment rate has a much longer time period (which can be measured as 2 times the period from a trough to a peak) of fluctuations than the wage share. While the employment rate seems to have cycles running over centuries, the wage share displays cycles running over decades. On the other hand, the data generated by the Goodwin model (Figure 2) shows both the employment and the wage share to have fluctuations of similar time periods.

Second, in the actual data (Figure 1a), employment rate has a much larger amplitude of fluctuation than the wage share. While the employment rate seems to have amplitudes of roughly 10 percentage points, the wage share displays cycles with amplitudes of at most 5 percentage points. On the other hand, the data generated by the Goodwin model (Figure 2) shows the opposite. In Figure 2, employment rate has a lower (or similar) amplitude of fluctuation than (as) the wage share.[12]

It is of course true that the time series generated by the model (Figure 2) depends on

[11] Capital-output ratio is from https://cepr.org/voxeu/columns/us-capital-glut-and-other-myths

[12] Another obvious way in which the model's predictions are not correct is that the wage share goes above 1. Restrictions necessary to ensure that the wage share and the employment rate never goes above unity are introduced in a modified Goodwin model in Desai et al. (2006). Compared to the original Goodwin model, the time series patterns of the modified Goodwin model present an even worse match with patterns observed in the data.

(a) Time series plots of the employment rate and the wage share for the U.S. economy, 1950–2019.

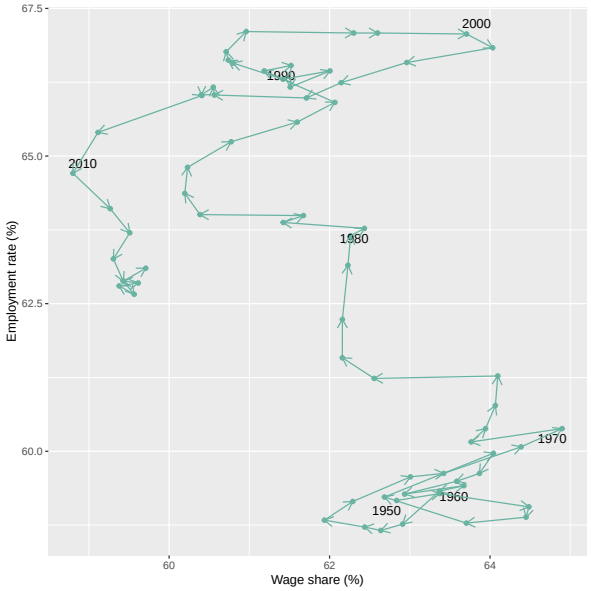

(b) Connected XY-plot of the employment rate and the wage share for the U.S. economy, 1950-2019.

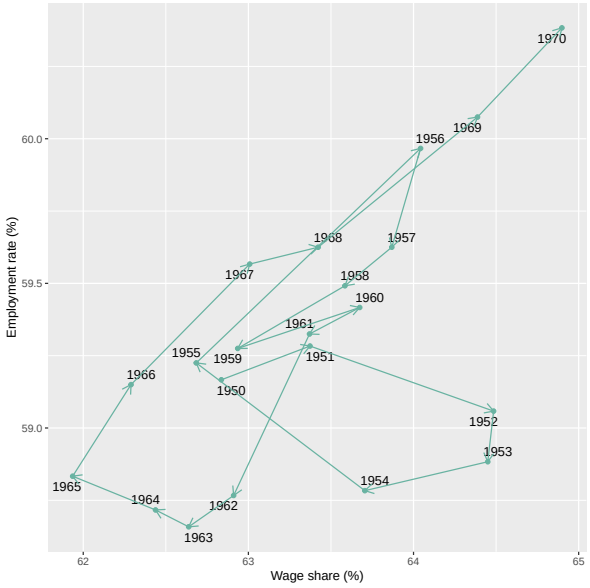

(c) Connected XY-plot of the employment rate and the wage share for the U.S. economy, 1950-1970.

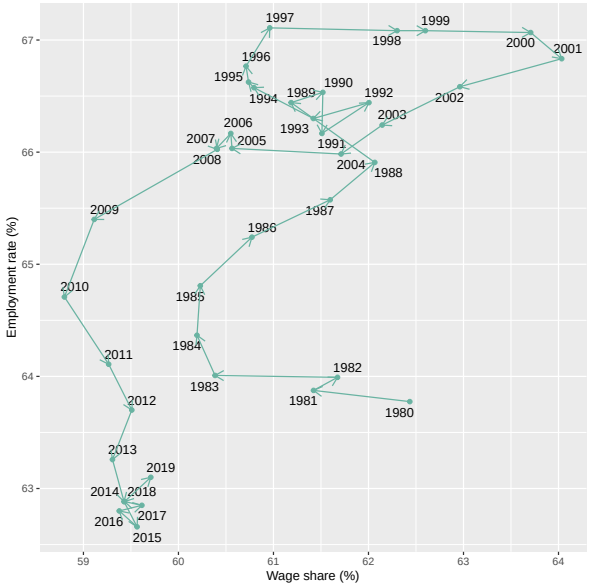

(d) Connected XY-plot of the employment rate and the wage share for the U.S. economy, 1980-2019.

Figure 1: Patterns observed in the data for the wage share and the employment rate in the U.S. economy, 1950-2019.

the parameter values. In particular, the parameters of the real wage Phillips curve, which are not observed, have an impact on the time period and amplitude of the fluctuations of the two series plotted in Figure 2. If ρ, which is the responsiveness of $\hat{w}$ (growth rate of the real wage rate) to v (employment rate), is increased, that increases the amplitude of fluctuations and reduces the time period of fluctuation of the wage share series. Getting these two features of the cycle to match the actual data is quite difficult.

Third, the Goodwin model implies *clockwise* movement of trajectories on the xy plane when the wage share is measured on the x-axis and the employment rate is measured on the y-axis (see section 4.3 for details). To see if this pattern is observed in the data, I have constructed connected XY plots in the wage share-employment rate space and present them in Figure 1b, 1c and 1d. The first (Figure 1b) uses the full time period of the data set, 1950-2019; the second (Figure 1c) plots for the sub-period, 1950-1970 and the last figure (Figure 1d) uses data for the sub-period, 1980-2019.

From Figure 1b we see that there are possibly two different cycles, one playing out in the 1950s and 1960s (with center at wage share = 63% and employment rate = 59%), and the second evolving in the period since the early 1980s (centered at wage share = 61% and employment rate = 65%). The period of the 1970s seems to be a transition between the two regimes. When we zoom into the period of the 1950s and 1960s (Figure 1c), we see interesting smaller cycles, all moving in clockwise directions. One cycle runs from 1950 to 1955 (centered at wage share = 63.5% and employment rate = 59%) and a bigger one seems to run from 1955 to 1970 (centered at wage share = 63.5% and employment rate = 59.5%).

When we zoom in the period since the early 1980s, we see a similar picture. There seems to be a clockwise cycle running from 1980 to 1988 (centered at wage share = 62% and employment rate = 65%), which is interrupted by another clockwise cycle playing out from 1988 to 2003 (centered at wage share = 62.5% and employment rate = 66.5%). But from the early 2000s, and especially since 2004, we see the emergence of a *counterclockwise*

cycle. This recent most cycle (centered at wage share = 60% and employment rate = 64%) seems to have completed half of the full cycle by 2019 and is contrary to the predictions of the Goodwin model.

On balance, the empirical evidence in favor of the Goodwin model is not very strong. The patterns observed in the data corroborates cyclical fluctuation of the wage share and the employment rate. The prediction about clockwise movement in the wage share-employment rate space is sometime seen in the data (the 1950s to the 1990s) and sometime the evidence is to the contrary (the period since the early 2000s). The amplitude and time periods of fluctuation are not consistent between the model's predictions and the data. One is forced to conclude that the basic Goodwin model, while intuitively appealing, does not match the actual data very well.

6 Conclusion

The popular Goodwin model of cyclical dynamics in capitalist economies demonstrate that the contradictions of capitalism produce endless fluctuation of the wage share and the employment rate around their stable equilibrium values (critical points), without ever settling down at that stable equilibrium. Since the model abstracts from demand-side issues, its economic significance is to demonstrate cyclical behavior in capitalist economies even in the absence of demand fluctuations.

Some of the existing proofs of closed-orbit trajectories of the solutions are either complicated and rely on real analysis (Flaschel, 1984) or, if based on calculus, lack the full details (Desai et al., 2006). In this paper, I have presented a much simpler proof based on Liapunov's second method and an even simpler proof that relies only on basic calculus (see the appendix). I have also studied the local behavior of the system near the stable critical point. In this case, we see that if the system starts near the stable equilibrium, the closed-orbit

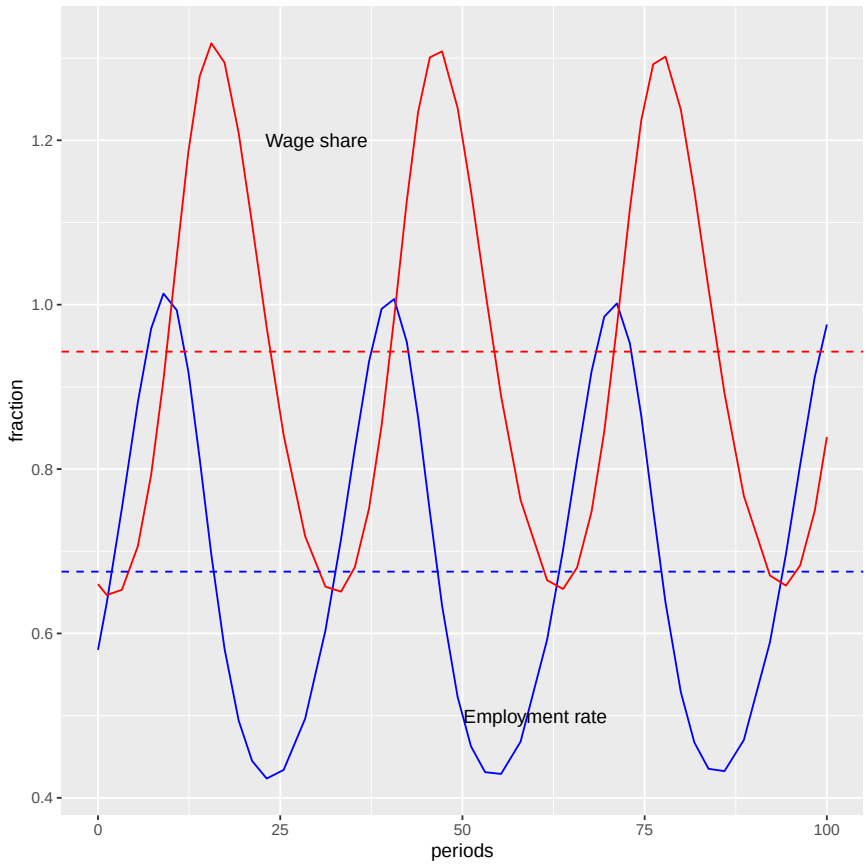

Figure 2: Time series plot of the employment rate (green bold) and the wage share (red bold) generated by simulating the Goodwin model with parameter values chosen to match data for the US economy since 1948. The dotted lines represent equilibrium values for the two variables: green for employment rate and red for wage share.

solution of the Goodwin model are ellipses.

While the Goodwin model presents an intuitively appealing explanation of cyclical fluctuations in capitalism, its specific predictions does not match the patterns observed in actual data very well, beyond the fact of cyclical fluctuations. Neither the time period nor the amplitudes of the fluctuations of the employment rate and the wage share emerging from the model seem to match what is observed in the actual data. Clockwise movement in the wage share-employment rate plane is observed for some time periods (which is in line with the predictions of the Goodwin model) but for other time periods counter-clockwise movement is observed (which is counter to the prediction of the Goodwin model). More work is needed to make the Goodwin model usable as a tool of analysis.

References

Binmore, K. G. (1991). *Mathematical Analysis: a straightforward approach*. Cambridge University Press, First Indian Edition, New Delhi, India.

Blecker, R. A. and Setterfield, M. (2019). *Heterodox Macroeconomics: Models of Demand, Distribution and Growth*. Edward Elgar, Cheltenham, UK.

Boyce, W. E. and DiPrima, R. C. (2009). *Elementary Differential Equations and Boundary Value Problems*. John Wiley & Sons, Inc., Hoboken, NJ, Ninth edition.

Desai, M., Henrya, B., Mosleya, A., and Pemberton, M. (2006). A clarification of the Goodwin model of the growth cycle. *Journal of Economic Dynamics & Control*, 30:2661–70.

Desai, M. and Ormerod, P. (1998). Richard Goodwin: A Short Appreciation. *The Economic Journal*, 108:1431–1435.

Flaschel, P. (1984). Some Stability Properties of Goodwin's Growth Cycle A Critical Elaboration. *Zeitschrift für Nationalökonomie / Journal of Economics*, 44:63–69.

Goodwin, R. M. (1967). A Growth Cycle. In Feinstein, C. H., editor, *Socialism, capitalism and economic growth: essays presented to Maurice Dobb*. Cambridge University Press.

Simon, C. P. and Blume, L. (1994). *Mathematics for Economists*. W. W. Norton & Company, New York, NY.

Skott, P. (2023). *Structuralist and Behavioral Macroeconomics*. Cambridge University Press, New York, NY.

Velupillai, K. (1979). Some Stability Properties of Goodwin's Growth Cycle. *Zeitschrift für Nationalökonomie / Journal of Economics*, 39:245–257.

A Alternative proof of closed orbit trajectories

Combining (6) and (7), which defines the re-parametrized Goodwin model, we get

$$\frac{du}{dv} = \frac{du/dt}{dv/dt} = \frac{[-\eta_2 + \theta_2 v]\, u}{[\eta_1 - \theta_1 u]\, v},$$

which becomes

$$\frac{[\eta_1 - \theta_1 u]}{u} du = \frac{[-\eta_2 + \theta_2 v]}{v} dv.$$

On integrating both sides and rearranging terms, we get

$$\eta_1 \ln u - \theta_1 u + \eta_2 \ln v - \theta_2 v = c_0, \tag{17}$$

where c_0 is a constant of integration. Collecting terms, we get

$$\ln u^{\eta_1} v^{\eta_2} = \theta_1 u + \theta_2 v + c_0$$

so that on exponentiating and rearranging, we get

$$u^{\eta_1} e^{-\theta_1 u} v^{\eta_2} e^{-\theta_2 v} = C,$$

where $C = e^{c_0}$. Thus, solutions trajectories satisfy the following equation

$$f(u)g(v) = C, \text{ where } f(u) = u^{\eta_1} e^{-\theta_1 u}, \text{ and } g(v) = v^{\eta_2} e^{-\theta_2 v}. \tag{18}$$

I will now show that (18) defines closed-orbit trajectories using a multi-step argument.

Step 1. Using the definition of the function f in (18) we see that $f(0) = 0$, $\lim_{u\to+\infty} f(u) = 0$, $f'(u) > 0$ if $0 \leq u < \eta_1/\theta_1$, $f'(u) = 0$ if $u = \eta_1/\theta_1$, and $f'(u) < 0$ if $u > \eta_1/\theta_1$. Hence, the function is increasing for $0 \leq u < \eta_1/\theta_1$, attains its *unique* maximum at $u = \eta_1/\theta_1$ (the maximum value of f on the nonnegative part of the real line is $M_1 = \eta_1^{\eta_1} (\theta_1 e)^{-\eta_1}$), and the function is decreasing for $u > \eta_1/\theta_1$.

In a similar manner, using the definition of the function g in (18) we see that $g(0) = 0$, $\lim_{v\to+\infty} g(v) = 0$, $g'(v) > 0$ if $0 \leq v < \eta_2/\theta_2$, $g'(v) = 0$ if $v = \eta_2/\theta_2$, and $g'(v) < 0$ if $v > \eta_2/\theta_2$. Hence, the function is increasing for $0 \leq v < \eta_2/\theta_2$, attains its *unique* maximum at $v = \eta_2/\theta_2$ (the maximum value of g on the nonnegative part of the real line is $M_2 = \eta_2^{\eta_2} (\theta_2 e)^{-\eta_2}$), and the function is decreasing for $v > \eta_2/\theta_2$.

Step 2. Because the maximum of f and g are unique, it implies that: (a) no nonnegative values of v and u can satisfy the equation

$$f(u)g(v) = C, \text{ if } C > M_1 M_2; \tag{19}$$

and (b) a unique solution $v = \eta_2/\theta_2$ and $u = \eta_1/\theta_1$ satisfies the equation

$$f(u)g(v) = C, \text{ if } C = M_1 M_2. \tag{20}$$

Step 3. Let $0 < \gamma < M_1$. Then, by the properties of f established in step 1, the equation $f(u) = \gamma$ has two solutions on the nonnegative part of the real line, u_1, u_2, such that $u_1 < \eta_1/\theta_1 < u_2$. Now consider the equation

$$g(v) = \frac{\gamma M_2}{f(u)}, \text{ where } \gamma < M_1. \tag{21}$$

Let us find solutions of (21) for all possible values of $u \geq 0$.

- If $0 \leq u < u_1$, then (21) has no solution. To see this, note that if $0 \leq u < u_1$, then $f(u) < \gamma$. Hence, $\gamma M_2/f(u) > M_2$. Thus, (21) has no solution (because M_2 is the unique maximum of g).

- If $u = u_1$, then $f(u) = \gamma$. Thus, (21) has only one solution: $v = \eta_2/\theta_2$; this follows from (20).

- If $u_1 < u < u_2$, then (21) has two solutions, $v_3(u), v_4(u)$, where $v_3(u) < \eta_2/\theta_2 < v_4(u)$. To see this, note that if $0 < u < u_1$, then $f(u) > \gamma$. Hence, $\gamma M_2/f(u) < M_2$. Thus, (21) has two solutions by the properties of g established in step 1.

- If $u = u_2$, then $f(u) = \gamma$. Hence, (21) has only one solution: $v = \eta_2/\theta_2$; this follows from (20).

- If $u > u_2$, then (21) has no solution. To see this, note that if $u > u_1$, then $f(u) < \gamma$. Hence, $\gamma M_2/f(u) > M_2$. Thus, (21) has no solution (because M_2 is the unique maximum of g).

We can conclude from this discussion that, for any value of $u \geq 0$, the equation (21) has at most two solutions. Note that finding the solutions of (21) is equivalent to finding solutions of (18) when solutions of the latter exist. Thus, we can conclude that (18) has at most two solutions for any $u \geq 0$. That is, a vertical line at any fixed value of u will intersect the solution trajectory at most two times. This implies that the solution trajectories that satisfy (18) cannot be spirals (because a vertical line at some values of u would intersect a spiral more than 2 times). Thus, we can conclude that the solution trajectories are closed orbits.[13]

[13]The proof of closed-orbit trajectories of a generalized Goodwin model in Desai et al. (2006, page 2665) is similar to what I have presented here, but it lacks the details.